# BUNDLE BRANCH BLOCKS SIMULATIONS IN VENTRICULAR MODEL WITH REALISTIC GEOMETRY AND CONDUCTION SYSTEM

**Elena Cocherová, Jana Švehlíková, Milan Tyšler**

Institute of Measurement Science, SAS, Bratislava, Slovakia

***Abstract***

*The goal of the study was to design a model of cardiac ventricles with realistic geometry that enables simulation of the ventricular activation with normal conduction system functions, as well as with bundle branch blocks. In ventricles, electrical activation propagates from the His bundle to the left and right bundle branches and continues to the fascicles and branching fibers of the Purkinje system. The role of these parts of the conduction system is to lead the activation rapidly and synchronously to the left and right ventricle. The velocity of propagation in the conduction system is several times higher than in the surrounding ventricular myocardium. If the conduction system works normally, QRS duration representing the total activation time of the ventricles lies in the physiological range of about 80 to 120 ms but it is more than 120 ms in the case of bundle branch blocks. In our study, the realistic geometry of the ventricles was constructed on the base of a patient CT scan, defining epicardial and endocardial surfaces. The first part of the conduction system (fast-conducting bundle branches, fascicles in the left ventricle and initial parts of the Purkinje fibers) was modeled as polyline pathways isolated from the surrounding ventricular tissue. The remaining part of the Purkinje system was modeled as an endocardial layer with higher conduction velocity. The propagation of the electrical activation in the ventricular model was modeled using reaction-diffusion (RD) equations, except for the first part of the conduction system, where the activation times were evaluated algebraically with respect to predefined velocity of propagation and estimated distance between the His bundle and particular entry point to the layer with higher conduction velocity. Propagation of activation in cardiac ventricles was numerically solved in Comsol Multiphysics environment. Several configurations of the first part of the conduction system with different number of polyline pathways and entry points were proposed and tested to achieve realistic activation propagation. For the model with 9 starting points, realistic total activation time (TAT) of the whole ventricles of about 108 ms was obtained for the model with normal conduction system, and realistic TAT of 126 ms and 149 ms were obtained for the right and left bundle branch block (RBBB, LBBB), respectively. Very similar TAT was found also for the model with 7 starting points, but unrealistically long TAT was obtained in LBBB simulation for the model with only 5 starting points.*

***Keywords***

*cardiac ventricles, reaction-diffusion model of activation propagation, conduction system, bundle branch blocks*

## Introduction

The proper heart function depends on appropriate and synchronous electrical activation of the heart. Disturbances of electrical activation of the ventricles may lead to decreased pumping function of the heart.

In the heart ventricles, the electrical activation starts from the atrioventricular node and propagates through the His bundle that further divides to the left and right bundle branches, anterior and posterior fascicles in the left ventricle and continues to the branching fibers of the Purkinje system. The fast-conducting His bundle, bundle branches, fascicles and Purkinje system create the conduction system and lead the activation to the working ventricular myocardium. The velocity of activation propagation in the conduction system is several times higher than in the working ventricular myocardium [1, 2].

Complete left or right bundle branch block (LBBB, RBBB) lead to prolongation of the total activation time and asynchronous function of the ventricles. Complete and incomplete bundle branch blocks (BBBs) and some other heart diseases and abnormalities have often similar ECG characteristics [3, 4]. Difficulties in the BBBs diagnostics relate to the position, size, and degree of tissue impairment in particular cases [5, 6].

The real propagation of the activation front in the heart tissue is dependent on tissue parameters, as well as on the front shape [7]. It can be mathematically modeled by using less time-consuming propagation models based on the fastest route algorithm [8], cellular automata [9, 10]



Lekar a technika – Clinician and Technology 2021, vol. 51(1–4), pp. 21–28, DOI: 10.14311/CTJ.2021.1.03
ISSN 0301-5491 (Print), ISSN 2336-5552 (Online)

or eikonal equations [11]. Most of the fast algorithms suppose constant propagation velocity in particular tissue, neglecting velocity changes caused by the activation front shape [12]. Propagation models using the reaction-diffusion (RD) equations (in monodomain or bidomain models of the tissue) [13, 14] preserve the velocity changes connected with activation front shape, however they are much more time-demanding than the abovementioned fast methods.

The local changes of electrical activity (action potential, AP) across cardiac cell membranes could be described by complex local models, including ion concentration changes and ion flux through various membrane channels [15]. Such local models include tens of ordinary differential and algebraic equations. These models are capable to model the shape of AP in detail, nevertheless their numerical solution is extremely time demanding.

More conventional way is to use simplified local model with limited number of equations, e.g., the FitzHugh-Nagumo (FHN) equations [13, 16, 17]. The FHN equations incorporate only two state variables and therefore they are more effective for application in RD model of activation propagation than other more complex local membrane models.

In our study, the geometry of ventricles model was constructed on the base of a patient CT scan. The conduction system in the ventricles was made up from two parts. The first one was modeled by polyline conductive pathways and comprised the His bundle, both bundle branches, fascicles in the left ventricle and initial parts of the Purkinje fibers. The second one represented the remaining part of the Purkinje fibers in both ventricles and was modeled as two endocardial layers with higher conduction velocity.

The left and right BBBs were modeled by disabling the first part of the conduction system in the particular ventricle. The activation propagation and the total activation times (TAT) when the whole ventricles were activated were computed and compared for models of normal activation as well as for the BBBs.

## Method

### Geometry of the realistic model

The geometry of the ventricles was obtained from a patient CT scan, where the outer epicardial surface and inner endocardial surfaces of the left and right ventricles were defined (grey in Fig. 1).

The height (base-to-apex dimension) of the ventricular model was approximately 130 mm (Fig. 1). The left-to-right dimension was approximately 140 mm, and the anterior-to-posterior dimension was 100 mm. The thickness of the ventricular wall was about 5–9 mm in the right ventricle and about 8–11 mm in the left ventricle in the middle of the model height.

### The first part of the conduction system model

In our study, the initial part of the conduction system (fast-conducting bundle branches, fascicles in the left ventricle and initial part of the Purkinje fibers) was modeled separately as polyline pathways isolated from the surrounding tissue. The His bundle (the upper line in the middle picture in Fig. 2) was further divided to the left and right bundle branches. Several configurations of the first part of the conduction system were designed: the model with nine polyline pathways and two models with reduced number of polyline pathways (Fig. 2–4).

### The second part of the conduction system model

The second part of the conduction system represented the remaining part of the Purkinje fibers in both ventricles. It was modeled as two endocardial layers with higher conduction velocity (referred as the fast-conducting Purkinje layers in Fig. 1, highlighted in green and blue).

The fast-conducting Purkinje layers at the endocardium of the ventricles were about 2 mm thick. The remaining volume of the ventricles represented the working ventricular myocardial (cardiac muscle) tissue with lower conduction velocity.

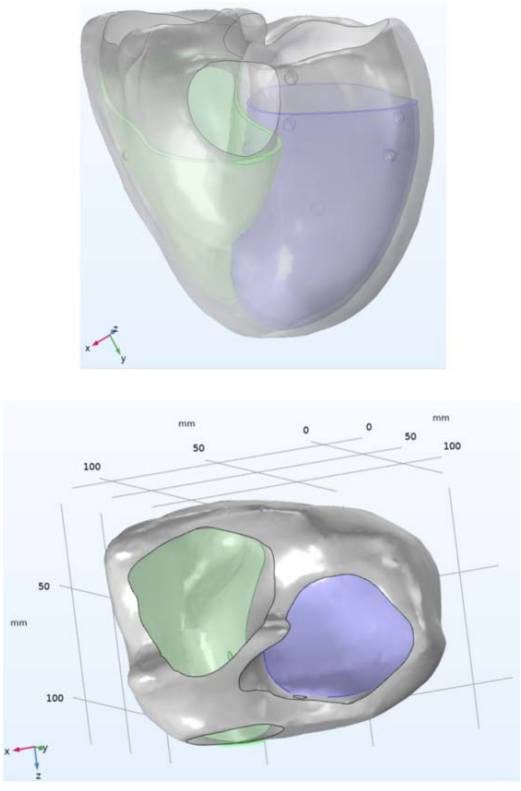


*Fig. 1: The ventricular model with realistic geometry: frontal view (top), base-to-apex view (bottom). The fast-conducting Purkinje layers in the right and left ventricle are highlighted in green and blue, respectively.*



Lekar a technika – Clinician and Technology 2021, vol. 51(1–4), pp. 21–28, DOI: 10.14311/CTJ.2021.1.03
ISSN 0301-5491 (Print), ISSN 2336-5552 (Online)

### Starting regions of activation

The activation can propagate from the first part of the conduction system model to the second one through the connections modeled as entry starting regions (SR). Each polyline pathway was ended in the SR through which the electrical activation passed into the Purkinje layer (Fig. 2). The positions of SRs were situated in the earliest activated areas of the ventricles as it was observed experimentally by Durrer [18].

In the model, the starting regions were located subendocardially, had approximately hemispherical shape and the centers of the spheres were located on the endocardial ventricular surface. The radius of the spheres was 3 mm.

### Starting activation times for the starting regions

The starting activation times in the SRs were evaluated algebraically with respect to a predefined velocity of propagation and the length of the particular polyline pathway.

The propagation velocity in the His bundle and the bundle branches was assumed $v = 1$ m/s and the velocity in the remaining parts of the polyline pathway was set to $v = 3$ m/s.

The propagation of activation in the conduction system is not visible in surface ECG signals, it can be observed as the QRS onset only after the activation starts spreading in larger volumes of the ventricular muscle tissue. Therefore, the shortest propagation time from the polyline pathways was found (starting region SR2) and subtracted from all SRs, to start the ventricular muscle activation in time zero.

Each relevant starting region was activated by the stimulation current at calculated starting activation time ($T_{st}$) as shown in Table 1. Only relevant activated SRs are numbered and colored with different colors in bottom parts in Fig. 2–4.

*Table 1: The starting activation times $T_{st}$ in conduction system models with 9, 7 and 5 starting regions.*

| | 9 regions | 7 regions | 5 regions |
|---|---|---|---|
| | $T_{st}$ (ms) | $T_{st}$ (ms) | $T_{st}$ (ms) |
| SR1 | 1.8 | 1.8 | 1.8 |
| SR2 | 0 | | |
| SR3 | 2.3 | 2.3 | 2.3 |
| SR4 | 15.7 | 15.7 | 15.7 |
| SR5 | 20.3 | 20.3 | 20.3 |
| SR6 | 21.3 | | |
| SR7 | 7.2 | 7.2 | |
| SR8 | 4.2 | 4.2 | |
| SR9 | 25.7 | 25.7 | 25.7 |

### Modeling of bundle branch blocks

The left and right BBBs were modeled by disabling all starting regions in the particular ventricle (Table 2).

The RBBB was modeled by omitting the starting regions in the right ventricle and LBBB was modeled by disabling all starting regions in the left ventricle.

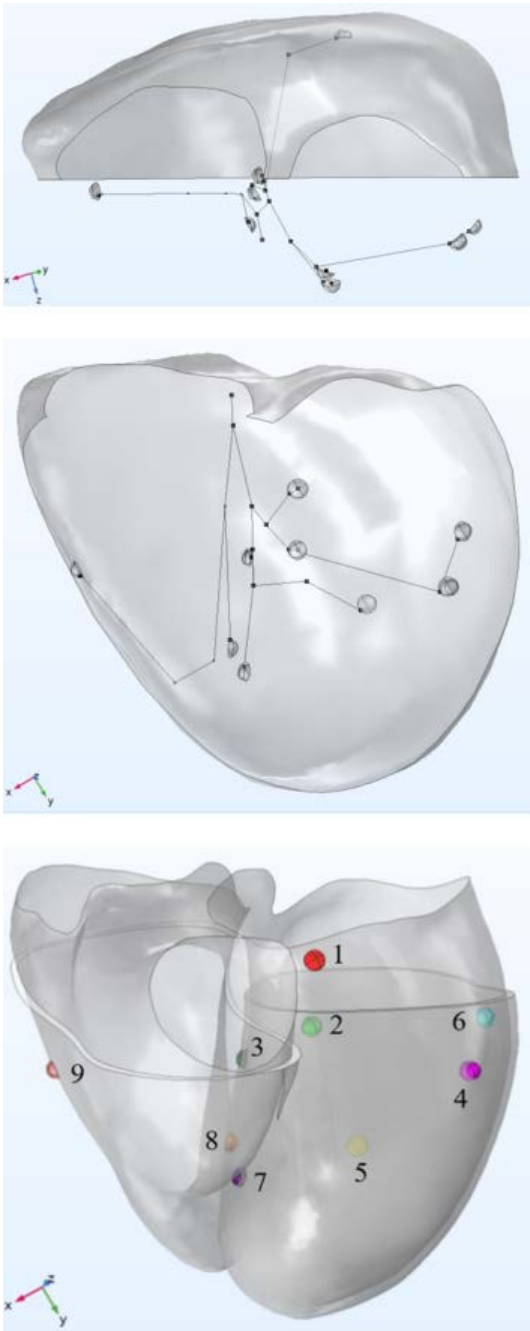


*Fig. 2: Top view (top) and fontal view (middle) of the initial part of the conduction system modeled by nine pathways and corresponding nine SRs (bottom).*



Lekar a technika – Clinician and Technology 2021, vol. 51(1–4), pp. 21–28, DOI: 10.14311/CTJ.2021.1.03
ISSN 0301-5491 (Print), ISSN 2336-5552 (Online)

*Table 2: Number of active starting regions in left and in right ventricle in models with 9, 7 and 5 starting regions for normal activation and BBBs simulation.*

| | 9 SRs | 7 SRs | 5 SRs |
|---|---|---|---|
| | RV / LV | RV / LV | RV / LV |
| Normal activation | 2 / 7 | 2 / 5 | 1 / 4 |
| RBBB | 0 / 7 | 0 / 5 | 0 / 4 |
| LBBB | 2 / 0 | 2 / 0 | 1 / 0 |

RV—right ventricle, LV—left ventricle.

If LBBB was simulated in the model with 9 or 7 polyline pathways, both SRs in the right ventricle were enabled (SR8 situated in the septum and SR9 situated in the free wall).

If LBBB was simulated in the model with 5 polyline pathways, only one SR was enabled for activation (SR9 situated in the free wall of the right ventricle).

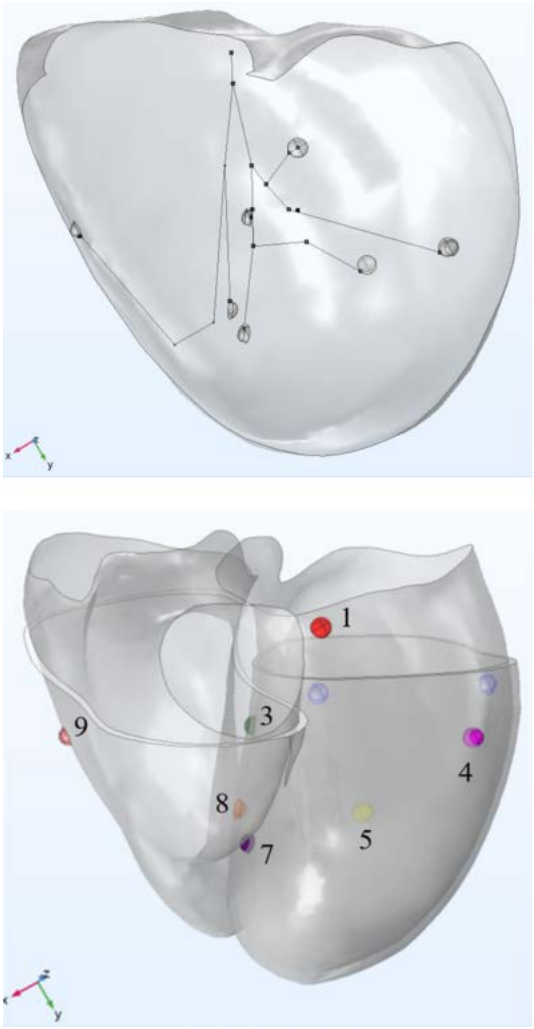


*Fig. 3: Fontal view of the initial part of the conduction system modeled by seven pathways (top) and corresponding seven SRs (bottom).*

**Reaction-diffusion model of activation propagation**

The RD propagation model was used to describe the propagation in the fast-conducting Purkinje layers and ventricular muscle tissue. The propagation of electrical activation in the monodomain RD model of the cardiac tissue [13, 17] is described by the partial differential equation:

$$\frac{\partial V_m}{\partial t} = \nabla \cdot \left( D \nabla V_m \right) - i_{ion} + i_s \qquad (1)$$

where $V_m$ is the membrane potential, $D$ is tissue diffusivity, $i_{ion}$ is the normalized local ionic transmembrane current density and $i_s$ is the normalized stimulation current density. Current densities are normalized to membrane capacitance with resulting units A/F. The normalized local ionic transmembrane current density $i_{ion}$ was represented by the modified FitzHugh-Nagumo (FHN) equations that determine the AP shape.

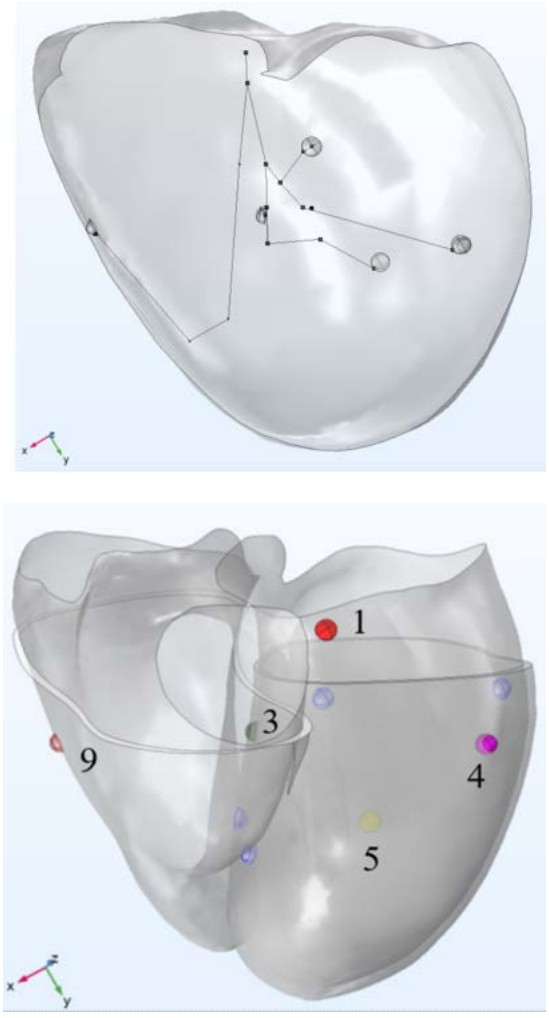


*Fig. 4: Fontal view of the initial part of the conduction system modeled by five pathways (top) and corresponding five SRs (bottom).*



Lekar a technika – Clinician and Technology 2021, vol. 51(1–4), pp. 21–28, DOI: 10.14311/CTJ.2021.1.03
ISSN 0301-5491 (Print), ISSN 2336-5552 (Online)

The parameter values in the modified FHN local model were taken from [13], with exception of the parameter governing the AP amplitude (0.12 V for the working myocardial tissue and 0.14 V for the Purkinje layer was used).

The pulse stimulation current $i_s$ (amplitude of the normalized stimulation current density was 100 A/F, duration of the stimulating pulse was 5 ms) was applied in activated SRs.

The tissue diffusivity $D$ relates to the tissue conductivity $\sigma$, the membrane surface-to-volume ratio $\beta$ and the membrane capacitance per unit area $C_m$:

$$D = \sigma/(\beta C_m). \qquad (2)$$

where $C_m = 1$ μF/cm$^2$ and $\beta = 1000$ cm$^{-1}$. The tissue diffusivity of the working myocardium in the ventricular model was set to $D = 0.0008$ m$^2$/s (relating to the tissue conductivity $\sigma = 0.8$ S/m). The tissue diffusivity of the fast-conducting Purkinje layers was set to $D = 0.0054$ m$^2$/s (relating to higher tissue conductivity $\sigma = 5.4$ S/m).

### Numerical computation

The partial differential RD equation describing the activation propagation and algebraic and ordinary differential equations related to FHN equations were numerically solved in Comsol Multiphysics. "Mesh Normal" with additional restriction to minimal and maximal mesh size (0.1 to 4 mm) was created for the ventricular model (Fig. 5).

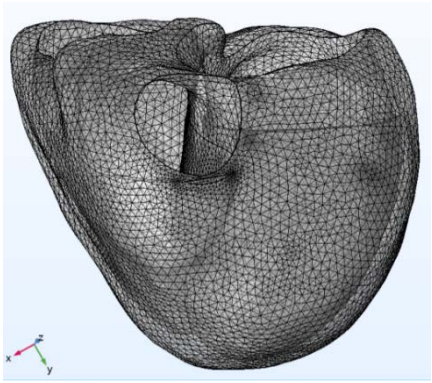

*Fig. 5: The geometry of the ventricular model covered with tetrahedral mesh.*

## Results

Spatial distributions of the membrane potential $V_m$ obtained for models with 9, 7 and 5 starting regions of activation are shown in Fig. 6–8. In the normal ventricular activation model with 9 starting regions in time $t$ = 20 ms (Fig. 6), the activation started and propagated from six SRs. Three starting regions (SR5, SR6 and SR9) were still inactive. In Fig. 7 the same model is shown in time $t$ = 57 ms, when the activation already started in all SRs and major part of the left ventricle was activated.

Spatial distributions of the membrane potential $V_m$ obtained for all models in time $t$ = 107 ms are shown in Fig. 8. The normal ventricular activation model with 9 SRs (top left) is just 1 ms before the activation of ventricles completed. When LBBB was simulated in models with 9 and 7 SRs (bottom left and middle), the activation fronts from SR8 and SR9 are going to meet in the right ventricle, while activation in the left ventricle is still not completed.

The total activation times when the whole ventricular models were activated are shown in Table 3. The shortest time was obtained for the normal activation model with 9 SRs (TAT = 108 ms). Normal activation models with 7 and 5 SRs had only very slightly longer TAT, so all tree models of the normal activation had realistic TATs. When RBBB was modeled, realistic TATs were achieved, and similar activation sequences were observed for all three models. When LBBB was modeled, realistic TATs were achieved for models with 9 and 7 starting regions (TAT = 149 ms in both cases). In both models the activation started from two SRs in the right ventricle (SR8 and SR9), therefore no difference was expected.

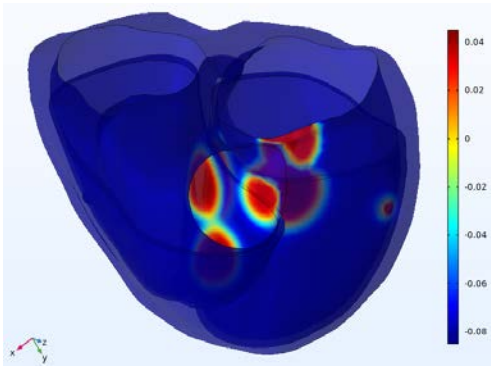


*Fig. 6: Spatial distribution of the membrane potential $V_m$ (V) in the normal ventricular activation model with 9 starting regions in time instant t = 20 ms.*

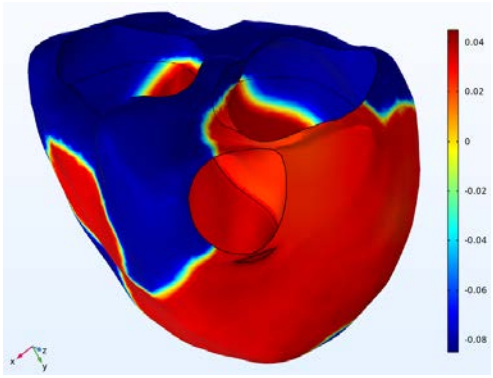


*Fig. 7: Spatial distribution of the membrane potential $V_m$ (V) in the normal ventricular activation model with 9 starting regions in time instant t = 57 ms.*



Lekar a technika – Clinician and Technology 2021, vol. 51(1–4), pp. 21–28, DOI: 10.14311/CTJ.2021.1.03
ISSN 0301-5491 (Print), ISSN 2336-5552 (Online)

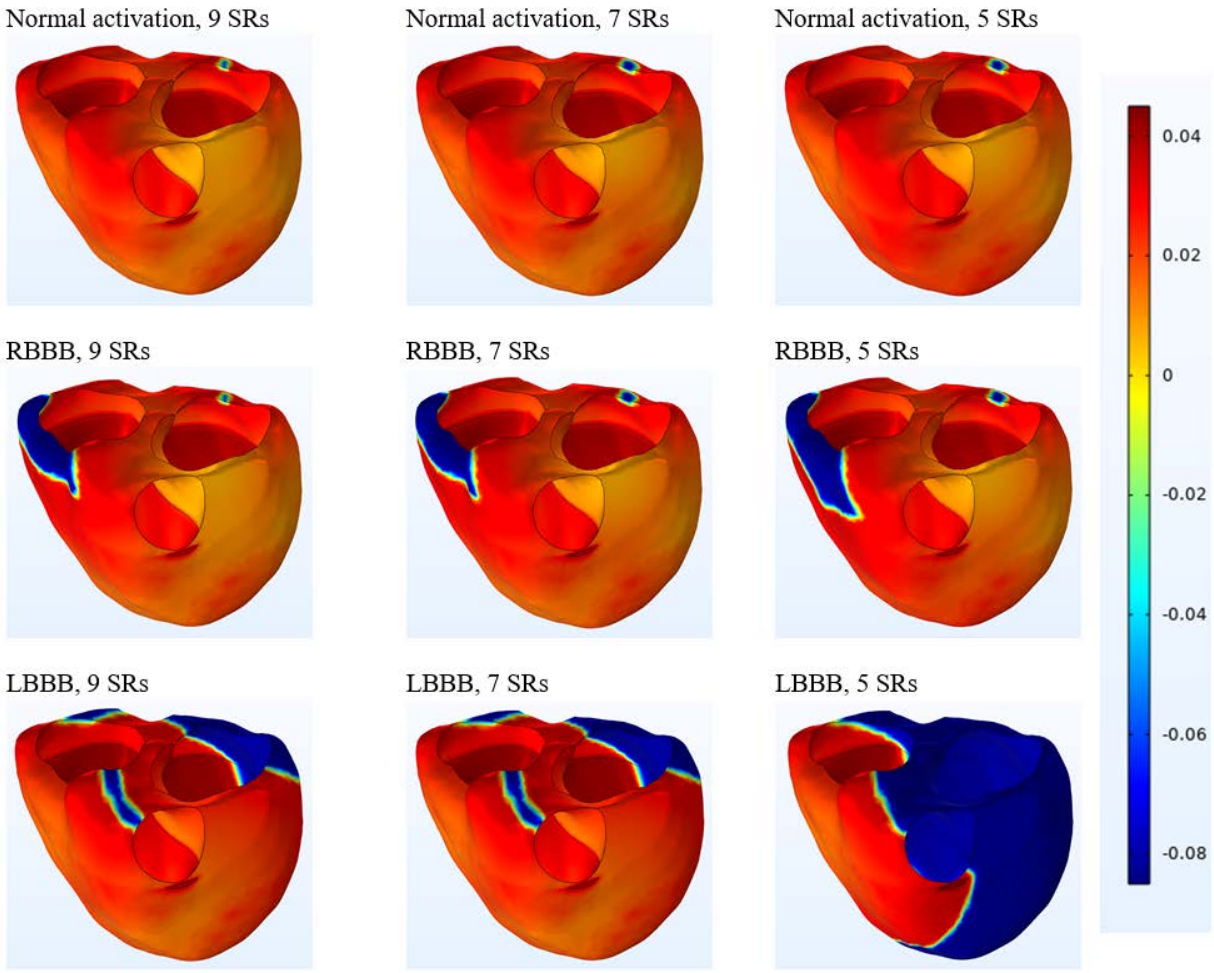


*Fig. 8: Spatial distribution of the membrane potential $V_m$ (V) in all ventricular models in time instant t = 107 ms.*

*Table 3: Total activation times (TATs) in conduction system models with 9, 7 and 5 starting regions.*

| | 9 SRs | 7 SRs | 5 SRs |
|---|---|---|---|
| | TAT (ms) | TAT (ms) | TAT (ms) |
| Normal activation | 108 | 109 | 110 |
| RBBB | 126 | 126 | 131 |
| LBBB | 149 | 149 | 205 |

However, when LBBB was simulated and model with 5 starting regions was used, unrealistically long TAT was obtained (TAT = 205 ms). This was caused by the reduction of SRs to only one (SR9), situated on the free wall of the right ventricle.

## Discussion

All three models of the conduction system with 9, 7 and 5 starting regions represented the ventricular activation satisfactorily when the normal activation of ventricles and RBBB were simulated. When LBBB was simulated, only two models with higher numbers of starting regions were appropriate. For the model with 5 SRs unrealistically long TAT was obtained. In this case, the activation started only in one starting region situated on the free wall of the right ventricle, what is inadequate. This resembles more an ectopic activation propagation when the activation is spreading from one pathological point and the TAT is correspondingly prolonged.

Negligible differences in the TATs were found for the models with 7 and 9 starting regions. Explanation of this is that the disabled SRs were always situated closely to other active starting regions.

In our ventricular model, the intrinsic anisotropy of the cardiac muscle tissue was not considered, therefore the transmural activation propagation and activation passing the septum between ventricles was not slowed, as it is in the real heart. Designed models will be used to simulate the activation of hearts with patient specific geometry and disorders of the conducting system. In patients (mainly with LBBB) indicated for cardiac resynchronization therapy (CRT) and implantation of CRT stimulation devices, the effects of different



Lekar a technika – Clinician and Technology 2021, vol. 51(1–4), pp. 21–28, DOI: 10.14311/CTJ.2021.1.03
ISSN 0301-5491 (Print), ISSN 2336-5552 (Online)

positioning of stimulating electrodes in the right and left ventricle and of their timing can be modelled before the implantation. The modelling could contribute to optimal planning of the resynchronization therapy by suggesting the most effective positions and timing of stimulating electrodes as well as to identifying of patients that might or might not respond to the therapy.

Nevertheless, further future improvement of the models, including involvement of the cardiac muscle anisotropy, simulation of local ischemia or scars can improve their accuracy and credibility.

## Conclusion

In our study, the ventricular models with realistic geometry and three configurations of the conduction system with 9, 7 or 5 starting regions of activation were created and tested for normal activation propagation and for simulation of bundle branch blocks. Activation propagation with realistic total activation times of 108 to 110 ms was obtained in all normal activation model configurations which corresponds to the expected interval of about 80–120 ms for normal activation of the heart ventricles.

Realistic TATs of 126 ms and 149 ms were obtained for the right and left bundle branch block, respectively, for models with 9 and 7 starting regions. For the model with only 5 SRs, unrealistically long TAT (205 ms) and ectopy-like activation propagation was obtained in LBBB simulation. Models with 9 or 7 starting regions were found to be equally appropriate for simulation of normal activation propagation and activations in case of BBBs.

## Acknowledgement

The work was supported by research grant VEGA 2/0109/22 from the VEGA grant agency and by grant APVV-19-0531 from the Slovak Research and Development Agency.

A preliminary version of the results published in this article was presented at the Trends in Biomedical Engineering 2021 conference.

## References

[1] Malmivuo J, Plonsey R. Bioelectromagnetism: Principles and applications of bioelectric and biomagnetic fields. Oxford: Oxford University Press; 1995. ISBN 0-19-505823-2.

[2] Macfarlane PW, van Oosterom A, Pahlm O, Kligfield P, Janse M, Camm J. Comprehensive electrocardiology. London: Springer-Verlag; 2011. ISBN 978-1-84882-046-3.

[3] Chan DD, Wu KC, Loring Z, Galeotti L, Gerstenblith G, Tomaselli G, et al. Comparison of the relation between left ventricular anatomy and QRS duration in patients with cardiomyopathy with versus without left bundle branch block. Am J Cardiol. 2014;113(10):1717–22. DOI: 10.1016/j.amjcard.2014.02.026

[4] Turagam MK, Velagapudi P, Kocheril AG. Standardization of QRS duration measurement and LBBB criteria in CRT trials and clinical practice. Curr Cardiol Rev. 2013;9(1):20–3. DOI: 10.2174/157340313805076269

[5] Boonstra MJ, Hilderink BN, Locati ET, Asselbergs FW, Loh P, van Dam PM. Novel CineECG enables anatomical 3D localization and classification of bundle branch blocks. Europace. 2021;23:80–7. DOI: 10.1093/europace/euaa396

[6] Galeotti L, van Dam PM, Loring Z, Chan D, Strauss DG. Evaluating strict and conventional left bundle branch block criteria using electrocardiographic simulations. Europace. 2013;15(12):1816–21. DOI: 10.1093/europace/eut132

[7] Clayton RH, Bernus O, Cherry EM, Dierckx H, Fenton FH, Mirabella L, et al. Models of cardiac tissue electrophysiology: Progress, challenges and open questions. Progress in Biophysics & Molecular Biology. 2011;104:22–48. DOI: 10.1016/j.pbiomolbio.2010.05.008

[8] van Dam PM, Oostendorp TF, van Oosterom A. Application of the fastest route algorithm in the interactive simulation of the effect of local ischemia on the ECG. Med Biol Eng Comput. 2009;47(1):11–20. DOI: 10.1007/s11517-008-0391-2

[9] Bacharova L, Szathmary V, Mateasik A. Electrocardiographic patterns of left bundle-branch block caused by intraventricular conduction impairment in working myocardium: a model study. Journal of Electrocardiology. 2011;44(6):768–78. DOI: 10.1016/j.jelectrocard.2011.03.007

[10] Cocherová E, Švehlíková J, Zelinka J, Tyšler M. Activation propagation in cardiac ventricles using homogeneous monodomain model and model based on cellular automaton. Measurement 2017: 11th International Conf. on Measurement; Bratislava: IMS SAS; 2017. ISBN 978-80-972629-1-4. DOI: 10.23919/MEASUREMENT.2017.7983575

[11] Pezzuto S, Kal'avsky P, Potse M, Prinzen FW, Auricchio A, Krause R. Evaluation of a rapid anisotropic model for ECG simulation. Front Physiol. 2017;8:265. DOI: 10.3389/fphys.2017.00265

[12] van Dam PM, van Oosterom A. Atrial excitation assuming uniform propagation. J Cardiovasc Electrophysiol. 2003;14: S166–71. DOI: 10.1046/j.1540.8167.90307.x

[13] Cocherová E. Analysis of the activation propagation velocity in the slab model of the cardiac tissue. Measurement 2015: 10th International Conference on Measurement; Bratislava: IMS SAS; 2015. ISBN 978-80-969672-9-2.

[14] Potse M, Dube B, Richer J, Vinet A, Gulrajani RM. A comparison of monodomain and bidomain reaction-diffusion models for action potential propagation in the human heart. IEEE Transactions on Biomedical Engineering. 2006;53(12):2425–35. DOI: 10.1109/tbme.2006.880875

[15] O'Hara T, Virag L, Varro A, Rudy Y. Simulation of the undiseased human cardiac ventricular action potential: Model formulation and experimental validation. Plos Computational Biology. 2011;7(5):29. DOI: 10.1371/journal.pcbi.1002061

[16] Cocherová E. Dependence of ventricular action potential shape on FitzHugh-Nagumo model parameters. Technical Computing Prague 2017: Proceedings of 24th Conference; Prague: UCT; 2017. ISBN 978-80-7592-002-7.

[17] Sovilj S, Magjarevic R, Lovell NH, Dokos S. A simplified 3D model of whole heart electrical activity and 12-lead ECG generation. Computational and Mathematical Methods in Medicine. 2013:134208. DOI: 10.1155/2013/134208

[18] Durrer D, van Dam RT, Freud GE, Janse MJ, Meijler FL, Arzbaecher RC. Total excitation of the isolated human heart. Circulation. 1970;41(6):899–912. DOI: 10.1161/01.CIR.41.6.899

*Elena Cocherová, Ph.D.*
*Department of Biomeasurements*
*Institute of Measurement Science*
*Slovak Academy of Sciences*
*Dúbravská cesta 9, 841 04 Bratislava*

*E-mail: elena.cocherova@savba.sk*
*Phone: +421 915 484 264*